A Study on the Cure Characteristics of Epoxy/Diaminodiphenylmethane System Prepared at Room Temperature

Fatemeh Ferdowsian,[1] Morteza Ebrahimi,[1] Ali Jannesari[2]

[1]*Department of Polymer Engineering and Color Technology, Amirkabir University of Technology, Tehran, Iran*
[2]*Department of Resins and Additives, Institute for Colorants, Paints, and Coatings, Tehran, Iran*

Received 13 October 2009; accepted 16 March 2010
DOI 10.1002/app.32545
Published online 11 June 2010 in Wiley InterScience (www.interscience.wiley.com).

ABSTRACT: The curing behavior and kinetics of epoxy resin with diaminodiphenylmethane (DDM) as the curing agent was studied by many researchers, however all of them prepared the system at a high-temperature condition (i.e., $T \geq 80°C$). In this study, a mixture of epoxy/DDM was prepared at ambient temperature and its curing characteristics were studied by using differential scanning calorimetry (DSC). The autocatalytic model was used to calculate the kinetic factors in the dynamic experiments. The kinetics of the curing reaction was also evaluated by two different isoconversional models; namely Friedman method and the Advanced Isoconversional method proposed by Vyazovkin to investigate the activation energy behavior during the curing reaction. The activation energy of the curing reaction was found to be in the range of 48 $\pm$ 2 kJ/mol and might be considered to be constant during the curing. In fact, our findings were different from the result reported by other researchers for the system which was prepared at elevated temperature. Therefore, it seems that the preparation temperature of the samples influenced considerably on the curing behavior of epoxy with DDM. Finally, a time–temperature–transformation (TTT) diagram was established to determine the cure process and glass transition properties of the system. © 2010 Wiley Periodicals, Inc. J Appl Polym Sci 118: 2092–2099, 2010

Key words: epoxy resin; diaminodiphenylmethane; differential scanning calorimetry; reaction kinetics; glass transition temperature; time–temperature–transformation diagram

INTRODUCTION

Epoxy resins are among the most versatile thermosetting systems, because of their outstanding properties and wide range applications. These resins usually out-perform most other resin types in terms of great chemical, moisture and solvent resistances, good thermal and dimensional stabilities, high adhesion strength to most substrates and superior electrical properties, which leads to their almost exclusive use in industrial coatings, adhesives, electronics, and high performance composites.[1–5]

Epoxy resins can be cured with different kinds of curing agents. Among these, the amine cured epoxy resin systems are frequently used in many applications so these systems attract great interest.[6]

Both aromatic and aliphatic amines are widely used as curing agents for epoxy resins. Aromatic amines are usually dedicated to composites, molding compounds, and castings. They offer cured epoxy structures with good heat and acid resistance. The primary advantages of aromatic amines over aliphatic amines for curing epoxy resins are the longer pot life as well as the development of higher heat resistance and greater chemical resistance; however, most of them are solids at room temperature and generally require heat for processing as well as for cure. The added heat required for mixing and cure increases the dermatitis and toxicity potential by releasing irritating vapors. On the other hand, it is not possible to fulfill any preheating process for the mixing of epoxy-based compounds with curing agent for most coating application methods. In this study, we investigated the effect of the temperature at which an epoxy resin was mixed with an aromatic amine before curing reaction on its cure characteristics.

4,4′-Diaminodiphenylmethane (DDM) has been considered as an aromatic amine component to react with diglycidyl ether of bisphenol A (DGEBA) and to form a thermoset structure. In thermoset systems, the kinetic features usually influence on the structure-property-processing relationships and therefore the material manufacturing and its utilization.[7] Hence, there are several studies on the curing behavior of DGEBA/DDM system and its properties. Liu et al.[7] have investigated the curing kinetics of DGEBA/DDM curing system and proposed a mechanistic model. Seo and Kim[8] and Bajaj et al.[9] studied

Correspondence to: M. Ebrahimi (ebrahimi@aut.ac.ir).

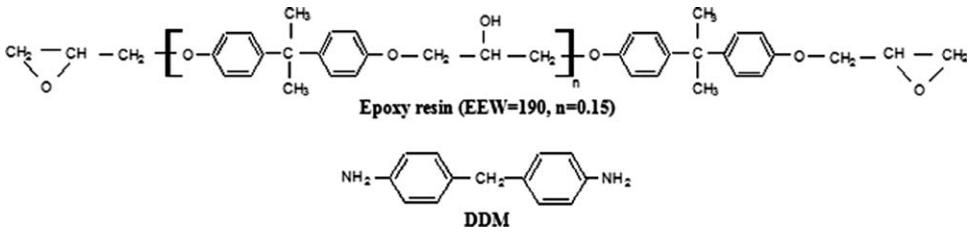

Figure 1 The chemical structure of the raw materials.

the curing behavior of an epoxy composite system composed of DGEBA with DDM. In both studies, it was found that the curing rate of the DGEBA/DDM system increased more or less with the increasing of filler content. Mercado et al.[10] have compared the DGEBA/DDM curing system with the curing system of DGEBA with two phosphorus-containing amine compounds. Schawe[11–13] evaluated the curing of DGEBA/DDM by using a temperature-modulated differential scanning calorimetry. It was shown, due to the vitrification process, the kinetics change from chemically-controlled to diffusion-controlled and also a new relationship for the conversion dependence of the glass transition temperature was derived. In the other researches, the effect of curing conditions on the glass transition temperature of cured DGEBA/DDM system was studied,[14–17] and the relationship of the glass transition temperature with the extent of conversion was derived.

To the best of our knowledge, the works which have considered on the DGEBA/DDM system, prepared their samples at elevated temperatures (i.e., higher than 80°C). In this work, we have studied the curing behavior of a sample of liquid epoxy resin (i.e., DGEBA), which mixed with DDM at room temperature. The cure kinetics of the system was performed by nonisothermal differential scanning calorimetry (DSC). The experimental results were analyzed by isoconversional and model fitting method.

EXPERIMENTAL

Materials

The materials used in this investigation were a DGEBA-based epoxy resin and diaminediphenylmethane (DDM) as curing agent. The epoxy equivalent weight (EEW) of the epoxy resin which was supplied by Huntsman was about 190. DDM was obtained from BASF. The materials were used as received. The chemical structures of the raw materials are shown in Figure 1.

Sample preparation

Two processes were used to prepare the samples. In the first method, a stoichiometric amount of the epoxy resin and DDM was mixed at room temperature named as RTM. The second method was a melt process in which the curing agent was melted at 80°C and then mixed with the epoxy in a stoichiometric ratio, which was named elevated temperature mixed (ETM) sample. Finally, the sample was cooled to the room temperature.

Characterization

To investigate the curing behavior of the epoxy-amine systems, a Perkin-Elmer Pyris 6 instrument was used. The experiments were carried out under nitrogen flow of 50 mL/min. The samples weight used in these experiments ranged from 2–3 mg. In dynamic modes, the samples were heated from 25 to 270°C at four different heating rates (i.e., 2.5, 5, 7.5, and 10°C/min) to follow the heat evolution due to the chemical reaction occurring in these conditions. The isothermal experiments were conducted at four temperatures namely 90, 110, 130, and 150°C. In the case of isothermal experiments, the thermal program was imposed by jumping to the cure temperature using a heating rate of 60°C/min. After the completion of curing, the samples were cooled to 20°C at 10°C/min to minimize the enthalpy relaxation in the next heating rate. Finally, the last scan was performed at 10°C/min heating rate to investigate the glass transition behavior of cured systems and to determine the residual heat of reaction.

Optical microscopic studies were performed with a Leitz DMR polarizing microscope, to study the homogenity of the samples before the curing step.

To study the structure of the samples, FTIR and H-NMR analyses were carried out. FTIR spectra of the samples were prepared using a Perkin-Elmer Spectrum One instrument. H-NMR spectra were measured at room temperature on a Brucker AV400 spectrometer operating at 400 MHz, using deuterated dimethylsulphoxide (DMSO-d6) as a solvent.

The gel point of the system was determined by using a MCR300 (Anton Paar) equipped with parallel plates with a 1 mm spacing. The measurement was done in dynamic mode with a heating rate of 10°C/min, a strain of 10%, and an oscillating frequency of 1 Hz.

Dynamic mechanical data were obtained using a DMA2980 TA instrument. Shear moduli were measured in oscillating bending, at a frequency of 1 Hz and strain amplitude of 1% of the length of the samples. Epoxy samples were heated from 30°C to 250°C using 5°C/min steps. Sample dimensions for DMA testing were 12 mm × 16 mm × 3 mm. In addition, the average molar mass between crosslinks was determined from DMA data by using eq. (1),[18]

$$M_c = \frac{\rho q R T}{G_e} \tag{1}$$

where M_c is the number average molar mass between crosslinks, q is the front factor (usually equal to 1[16]), ρ is the density at temperature T (K), G_e is the equilibrium modulus in the rubbery region at temperature T, and R is the universal gas constant.

KINETIC ANALYSIS

The reaction rate equations based on power law model usually consist of two different functions, namely temperature function [$k(T)$] and fractional conversion function [$f(\alpha)$] as showed in eq. (2),[19]

$$\frac{d\alpha}{dt} = f(\alpha)k(T) \tag{2}$$

The dependency of the rate constant, k, on the reaction temperature is traditionally described by Arrhenius equation. The function of fractional conversion [$f(\alpha)$] is usually estimated by terms of an autocatalytic mechanism.[20,21] The autocatalytic expression is proposed as in eq. (3)[22]:

$$\frac{d\alpha}{dt} = A \exp\left(\frac{-E}{RT}\right)\alpha^m(1-\alpha)^n \tag{3}$$

where A is the pre-exponential factor, E is the activation energy, R is the gas constant, T is the absolute temperature, m and n are reaction orders. To take into account the autocatalytic reaction, where the initial reaction rate of the autocatalytic reaction is not zero, Kamal proposed the generalized expression that is shown in eq. (4)[7]:

$$\frac{d\alpha}{dT} = (A_1 \exp\left(\frac{E_1}{RT}\right) + A_2 \exp\left(\frac{E_2}{RT}\right)\alpha^m)(1-\alpha^n) \tag{4}$$

In addition, isoconversional methods are usually used to study the activation energy behavior of the curing reaction precisely. These models allow us to evaluate the effective activation energy as a function of the extent of reaction. If changes in the cure mechanism are associated with the changes in the activation energy, they can be detected by using an isoconversional method.[8,23] The isoconversional principle states that the reaction rate at a constant extent of conversion is only a function of the temperature.[24] Isoconversional models can be treated in two different ways i.e., integral method and differential method.[25] In differential method, the common equation proposed by Friedman can be expressed as in eq. (5)[26]:

$$\ln\left(\beta\frac{d\alpha}{dT}\right)_{\alpha,i} = \ln[A_\alpha f(\alpha)] - \frac{E_\alpha}{RT_{\alpha,i}} \tag{5}$$

where β is the heating rate, the subscript i denotes to the ordinal number of nonisothermal experiments conduced at different heating rates and the subscript α denotes the quantities evaluated at a specific conversion degree. In this method, E_α is calculated from the slope of $\ln(\beta\frac{d\alpha}{dT})$ versus $1/T$ plot at a specific value of α.

One of the most accurate equations based on integral method is the advanced isoconversional method, which is proposed by Vyazovkin.[27,28] In this method, the reaction model is assumed to be independent of the heating program. According to this assumption, the J-integrals in each value of α are equal for all experiments that carried out under different arbitrary temperature programs, $T_i(t)$. The E_α value is determined as a value that minimizes the function φ [i.e., eqs. (6) and (7)],

$$\varphi(E_\alpha) = \sum_{i=1}^{s}\sum_{i\neq j}^{s}\frac{J(E_\alpha, T_i(t_\alpha))}{J(E_\alpha, T_j(t_\alpha))} \tag{6}$$

where

$$J(E_\alpha, T_i(t_\alpha)) = \int_{t_{\alpha-\Delta\alpha}}^{t_\alpha} \exp\left[\frac{-E_\alpha}{RT_i(t)}\right]dt \tag{7}$$

where the subscript i and j denote different heating rates, s is the total number of heating rates.[24]

RESULTS AND DISCUSSION

Kinetics parameters

In this work, the kinetic parameters of RTM sample curing were investigated, and the results were compared with the parameters were reported for ETM samples curing. DSC curves of the RTM sample cured at different heating rates are shown in Figure 2. The total curing heat is evaluated by the integration of exotherm peaks because the second heating of the cured samples did not show any residual heat of reaction, and the curing reactions could be assumed to be completed. The cure characteristics of

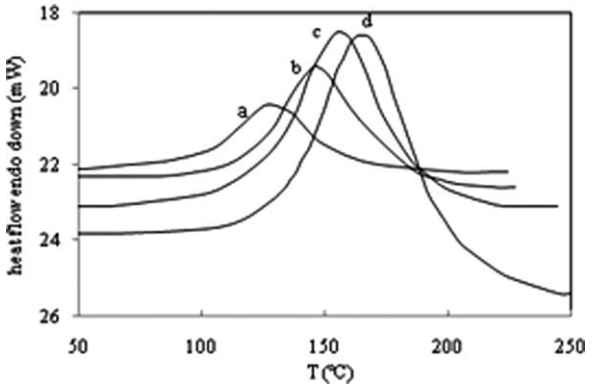

Figure 2 DSC curves of the RTM sample cured at different heating rates: (a) 2.5°C/min, (b) 5°C/min, (c) 7.5°C/min, and (d) 10°C/min.

RTM samples are shown in Table I. As can be seen, the total heat of reaction at different heating rates are almost the same and with increasing the heating rate, the onset temperature of reaction (T_{onset}), the termination temperature of reaction (T_{end}), and the temperature of exothermic peak (T_p) shift to higher temperatures.

The reaction kinetic parameters were determined by fitting the dynamic DSC conversion data to the autocatalytic equation [i.e., eq. (3)] by using the least square regression method. The obtained kinetic parameters are compiled in Table II. As can be seen, the activation energy and the overall reaction order are 54 kJ/mol and 1.8, respectively. Excellent agreement is observed between the calculated results and the experimental data in a broad temperature range as can be seen in Figure 3. In fact, this agreement was expected because the initial rates of RTM curing reactions at low temperatures were approaching to zero. Other researchers used Kamal's equation [eq. (4)] for the systems prepared at high temperatures (ETM).[8] They reported two activation energies for their ETM samples (i.e., 62 and 45 kJ/mol) and found out that the overall reaction order was 2. We also used Kamal's Equation for the DSC data of RTM sample. The kinetics behavior described by Kamal's equation does not agree with the experimental data in the early and last stages of curing reaction (Fig. 4). Therefore, it seems that the usual autocatalytic model (with one activation energy) can more accurately fit the experimental data. To investigate the accuracy of the obtained result with respect to the activation energy of RTM curing reaction, Friedman and Vyazovkin methods were used to evaluate the activation energy behavior during the curing reaction.

TABLE I
The Curing Characteristics of RTM Sample

Heating rate (°C/min)	T_{onset} (°C)	T_{end} (°C)	T_p (°C)	ΔH_{total} (J/g)
2.5	62.42	189.88	128	−656.5
5	74.22	220.11	147.35	−654.9
7.5	78.22	224.11	155.90	−656.6
10	104.76	242.02	165.51	−652.7

TABLE II
The Values of the Reaction Kinetic Parameters of RTM Sample Obtained by Applying Autocatalytic Model

Kinetic parameters	k (s^{-1})	E_a (kJ/mol)	n	m
	5.36×10^{7}	54	1.3	0.5

Based on Friedman method, the activation energies at different conversions are obtained by plotting $\ln(\beta \frac{d\alpha}{dT})$ versus $1/T$. Figure 5 shows this plot for our RTM experimental data and as can be seen a linear relationship is obtained, thus confirming the validity of the proposed model (i.e., ordinary autocatalytic model). Also, it can be observed that the activation energies at all conversions are nearly the same (ca. 48 ± 2 kJ/mol) which is in good agreement with the value obtained by using autocatalytic model.

In addition, the activation energy behavior was determined based on Vyazovkin equation [eq. (6)]. The results are presented in Figure 6. It shows that the activation energies in all fractional conversions are about 47 ± 2 kJ/mol which approves the Friedman results.

To find out the possible cause for the different behavior of the two samples, an optical microscopy, FTIR, and H-NMR analysis were carried out before curing step. The first probability of this difference could be related to the homogeneity of the system prepared at room temperature, hence the polarized optical microscopy was used for both samples and the optical micrographs are shown in Figure 7. The result revealed that the mixture was completely homogenous, the same as the ETM sample. It was actually expected because the solubility parameters of epoxy resin and DDM are the same [i.e., 20 $(J/cm^3)^{0.5}$].[29]

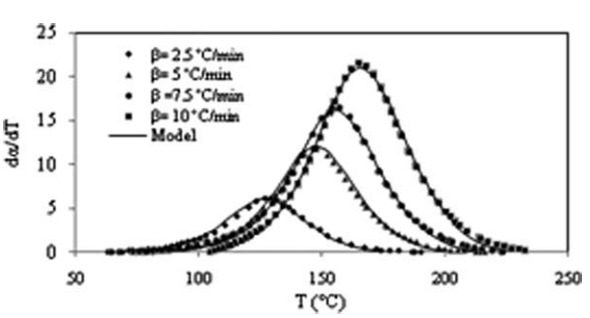

Figure 3 Comparison of experimental data of RTM sample with the autocatalytic model at different heating rates.

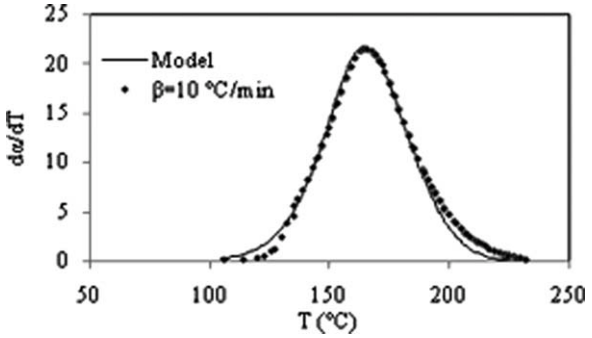

Figure 4 Comparison of experimental data of RTM sample with Kamal's equation at a 10°C/min heating rate.

Another probability of this difference could be related to the rearrangement of the chemical structure of the two samples during the preparation step. The FTIR spectra of RTM, ETM, and DDM are shown in Figure 8. By the comparison of RTM and ETM spectra, one can notice a slight change in the two regions of the wave number (about 1600 and 3400 cm^{-1}) that are related to amine bonds. It can be observed that the wave numbers related to amine bonds shifted to a lower wave number for the ETM sample. These shifts might be attributed to a hydrogen bond formation between DDM (NH-groups) and epoxy resin (epoxide groups).[30] In addition, for supporting our claim, the H-NMR analysis was also examined. The H-NMR spectra of RTM, ETM samples, DGEBA, and DDM are shown in Figure 9. It can be observed that all the resonance signals have been attributed to the corresponding protons of the DGEBA and DDM structures. By the comparison of RTM and ETM spectra, one can notice a slight change in some regions that might be attributed to NH-groups of DDM and epoxide groups. Because the high temperature made the reactive groups closer and facilitate the curing reaction of ETM. The

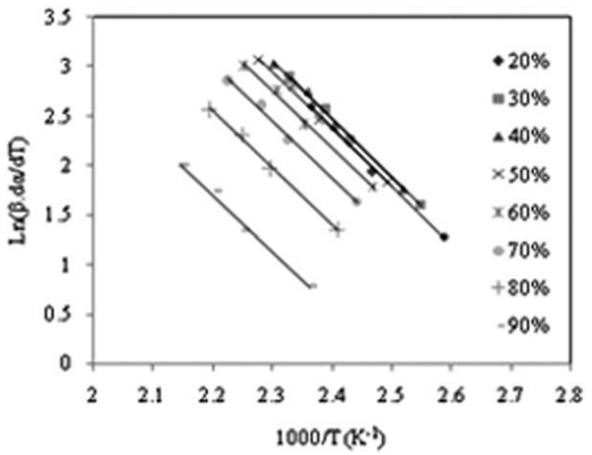

Figure 5 Friedman plots of $\ln(\beta\frac{d\alpha}{dT})$ versus $1/T$ for dynamic curing reaction of RTM sample.

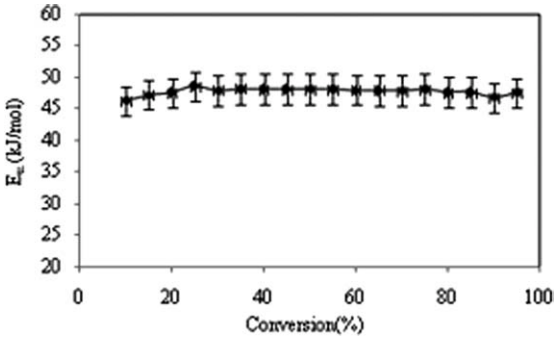

Figure 6 The dependency of the activation energy on the extent of conversion for the RTM sample from Vyazovkin method.

DSC results (Fig. 10) are also supporting justification, because the onset reaction temperature of the ETM sample was found to be lower (ca. 7°C) than the one for RTM sample. Hence, the initial rate of curing reaction of ETM is not zero, in contrast to the one for RTM, and the best model for describing the curing reaction can be Kamal's equation.

PHYSICAL PROPERTIES AND CURING PROCESS

In this section, the glass transition temperature of the cured RTM sample is reported as one of the most important physical properties and its dependency on the conversion is revealed. Moreover, to analyze and design the curing conditions of this

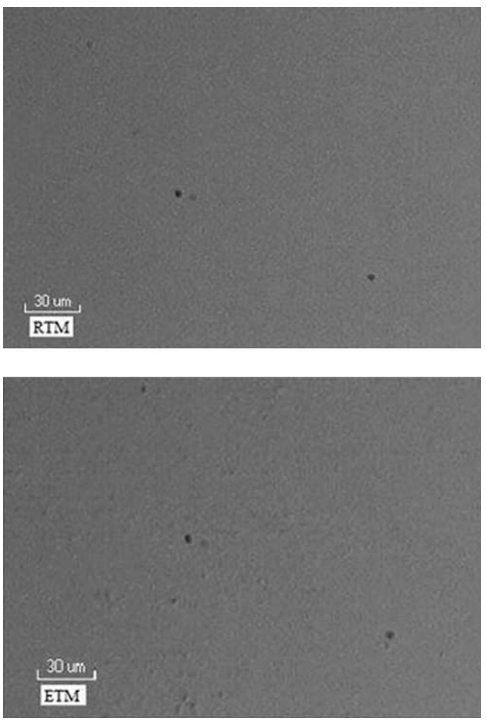

Figure 7 The polarized optical micrographs of RTM and ETM samples.

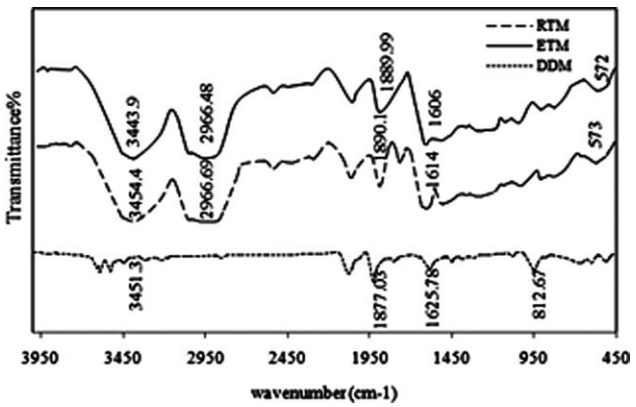

Figure 8 The FTIR spectra of ETM, RTM samples, and DDM.

system a time, temperature, transformation (TTT) diagram is developed.

Glass transition temperature

During the curing of a thermoset resin, the glass transition temperature, T_g, increases. Consequently, T_g rises from the glass transition temperature of the unreacted mixture to the glass transition temperature of the fully cured system. There is always a one to one relationship between glass transition temperature and the extent of conversion. To determine the relationship between the glass transition temperature and the extent of reaction, a series of isothermal DSC analysis were performed. In these experiments, the samples were cured at different periods of time (i.e., 1–13 min) and cooled to room temperature at a rate of 10°C/min. Then these samples scanned in the DSC setup from 25 to 250°C at the heating rate

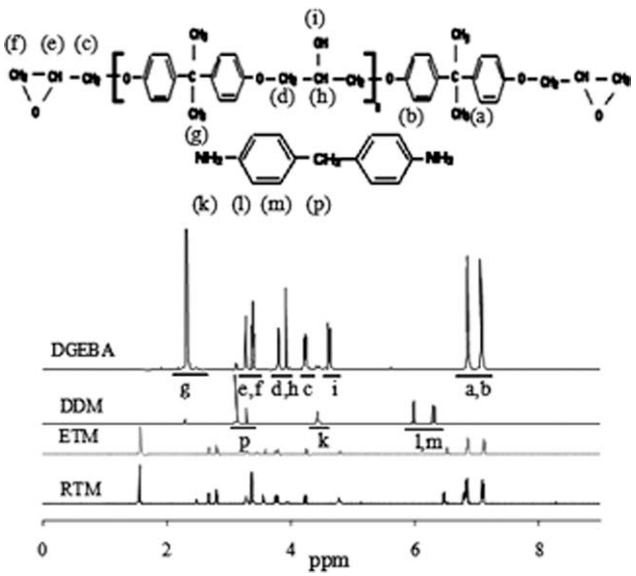

Figure 9 The H-NMR spectra of ETM, RTM sample, DGEBA, and DDM.

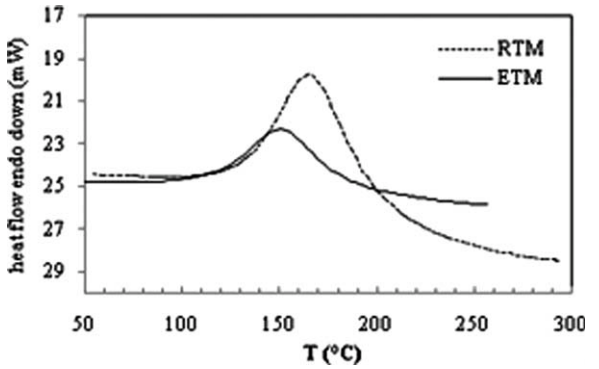

Figure 10 Comparison of DSC curves for RTM and ETM samples at a 10°C/min heating rate.

of 10°C/ min. The results are shown in Figure 11. As can be seen, the glass transition temperature of fully cured samples prepared at ambient temperature is about 122.7°C, which is considerably less than the one reported for ETM samples (i.e., 169°C). The difference between the glass transition temperature of RTM and ETM samples is related to the different crosslinked structures of both samples. For supporting our claim, the FTIR analysis was examined for both cured RTM and ETM samples and the spectra are shown in Figure 12. As can be observed the spectra have a significant difference at 1000–1300 cm^{-1} wavenumber that related to the ether bonds. This result confirms that some etherification reaction was occurred in the ETM sample, while this was not happened for the RTM sample (it is in line with the constant value of activation energy in the whole range of conversion, based on isoconversional analysis). Therefore the degree of crosslinking would be higher for ETM sample in comparison with RTM system. Worth mentioning that T_g can be attributed to conversion by using the DiBenedetto equation expressed in eq. (8)[31]:

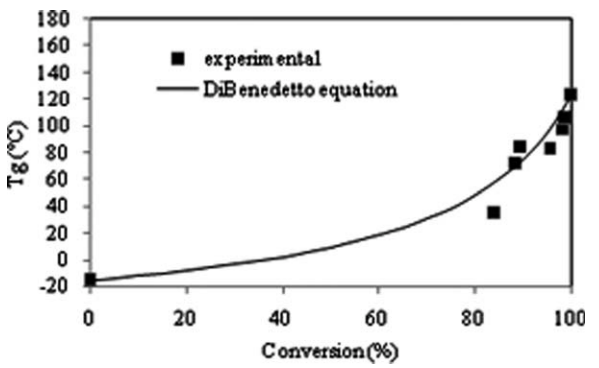

Figure 11 The evolution of the glass transition temperature as a function of the extent of reaction for the RTM sample.

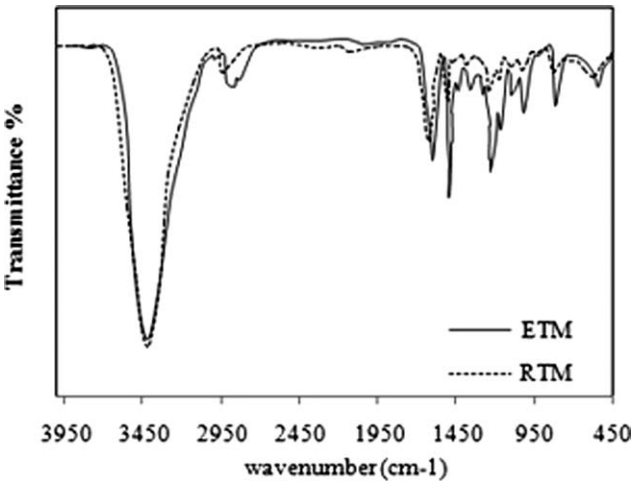

Figure 12 The FTIR spectra of cured ETM and RTM samples.

$$T_g = T_{g0} + \frac{(T_{g\infty} - T_{g0})\lambda\alpha}{1 - (1 - \lambda)\alpha} \quad (8)$$

where α is the fractional conversion, T_{g0} and $T_{g\infty}$ are the glass transition temperatures of uncured and fully cured system, respectively. This model employs the ratio of segmental mobility for crosslinked and uncrosslinked polymers, λ, to fit the model curve to the experimental data.[32] When we fitted the experimental results to this equation, the best value for λ was found to be 0.215, which is clearly lower than the value of λ reported for ETM sample (i.e., λ = 0.485).[7] The higher value of λ (for ETM samples) indicates that the mobility of uncrosslinked segments is lower or the mobility of crosslinked segments is higher. The decrease of uncrosslinked segment mobility can be confirmed with formation of hydrogen bonding as observed by FTIR results. In addition, to investigate the mobility of crosslinked segments, a DMA analysis was carried out for both samples.

The obtained DMA curves for the samples are shown in Figure 13. As discussed before, the average molar mass between crosslinks was measured by

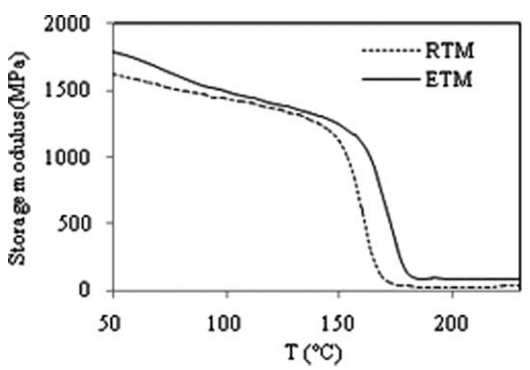

Figure 13 The DMA curves for RTM and ETM samples.

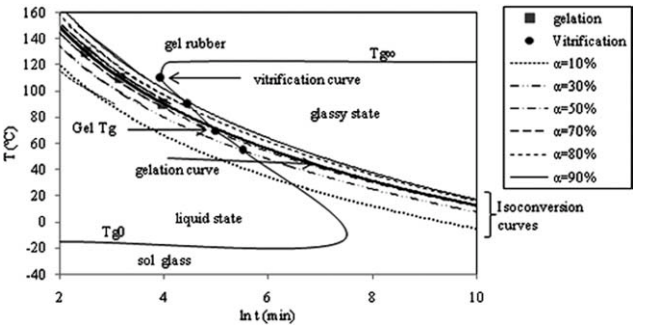

Figure 14 TTT isothermal cure diagram for RTM sample.

employing rubber elasticity theory [eq. (1)]. Based on this equation, the values of M_c for RTM and ETM samples were calculated to be 168.7 and 138.9 g/mol, respectively, which confirmed the above mentioned claim. In addition, as can be observed, the modulus of the rubbery region of RTM sample was less than ETM sample. This reduction in the modulus may be due to the reduction of matrix crosslink density (XLD), which again approves the mentioned justification and it can be assumed that about 20% of crosslinked structure of ETM system is related to the ether structure.

TTT diagram

To describe the different events (including gelation and vitrification) occur during curing, a general concept of a time, temperature, and transformation (TTT) diagram was established and developed to understand the curing process and glass transition properties of the system. The TTT diagram that was constructed for RTM sample is shown in Figure 14. The isothermal curves of TTT diagram were obtained from the isothermal DSC data which are shown in Figure 15.

A rheological analysis was also used to determine the gel point (Fig. 16). In this work, gelation was assumed to occur when the dynamic complex

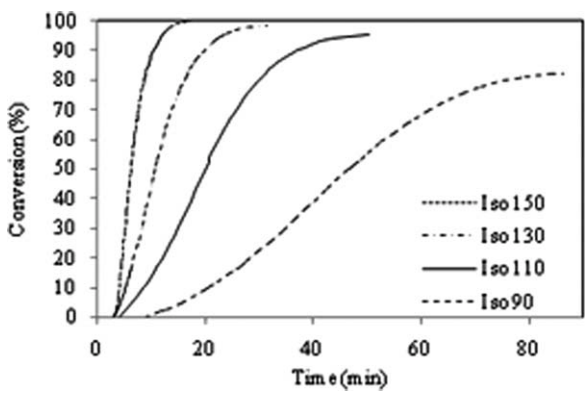

Figure 15 Conversion–time curves for RTM at different curing temperatures.

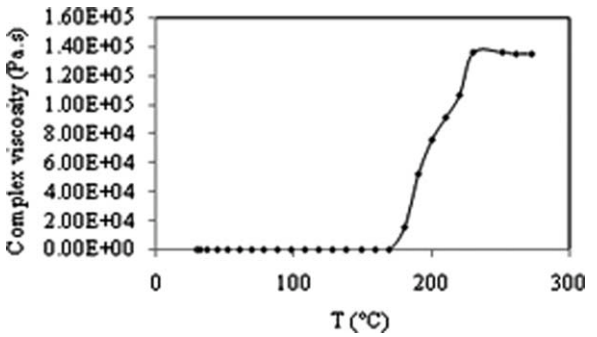

Figure 16 The change of the complex viscosity during the curing of RTM.

viscosity diagram had its inflection points. Combining the dynamic rheological data with the fractional conversion data obtained by means of DSC, the value for the fractional conversion at the gel point was determined to be about 58% and consistent with the amount that was calculated from Flory's gelation theory (i.e., 57%).

During the isothermal curing, vitrification conversion (α_v) was calculated by using eq. (9), which is a rearranged form of eq. (8). After the calculating of α_v, the vitrification time was obtained by using the conversion curve in isothermal DSC analysis (i.e., Fig. 15).

$$\alpha_v = \frac{T_{\text{react}} - T_{g0}}{\lambda(T_{g\infty} - T_{\text{react}}) + (T_{\text{react}} - T_{g0})} \tag{9}$$

CONCLUSIONS

The obtained results revealed that the reaction behavior of the epoxy/DDM system prepared at ambient and elevated temperatures was considerably different from each other. The activation energy for the samples prepared at ambient temperature was found to be 54 kJ/mol (based on autocatalytic model) and 48 ± 2 kJ/mol (based on model free kinetics). The T_g of the sample prepared at low temperature was found to be 122°C which was clearly less than the one for sample prepared at high temperature (i.e., T_g = 169°C). Also the value of λ for sample prepared at elevated temperature was found to be higher than the one prepared at high temperature. The DMA results illustrated that the average molecular weight between crosslinks of RTM sample was more than that for ETM sample (168.7 and 138.9 g/mol, respectively) which is in agreement with the results obtained for λ. These results revealed that the preparation temperature of epoxy/DDM samples had a significant effect on the curing reaction behavior and subsequently on the glass transition temperature. Finally, critical temperatures such as T_{g0}, Gel T_g, and $T_{g\infty}$ were evaluated and a complete isothermal TTT cure diagram of epoxy/DDM system was constructed.

References

1. Teil, H.; Page, S. A.; Michaud, V.; Manson, J. A. E. J Appl Polym Sci 2004, 93, 1774.
2. Ivankovic, M.; Incarnato, L.; Kenny, J. M.; Nicolais, L. J Appl Polym Sci 2003, 90, 3012.
3. Tai, H. J.; Chou, H. L. Eur Polym J 2000, 36, 2213.
4. Barone, L.; Carciotto, S.; Cicala, G.; Recca, A. Polym Eng Sci 2006, 46, 1576.
5. Hedrick, J. L.; Yilgör, I.; Wilkes, G. L.; Mcgrath, J. E. Polym Bull 1985, 13, 201.
6. Bianchini, G. Waterborne and Solvent Based Epoxide and Their End User Applications; SITA Technology, Chichester; 1996.
7. Liu, G.; Zhou, X.; Zhao, B.; Wang, J.; Gao, J.; Qu, X.; Zhang, L. Macromol Theor Simul 2006, 15, 339.
8. Seo, K. S.; Kim, D. S. Polym Eng Sci 2006, 46, 1318.
9. Bajaj, P.; Jha, N. K.; Ananda Kumar, R. J Appl Polym Sci 1990, 40, 203.
10. Mercado, L. A.; Ribera, G.; Galià, M.; Cádiz, V. J Polym Sci A Polym Chem 2006, 44, 1676.
11. Schawe, J. E. K. Thermochim Acta 2000, 361, 97.
12. Schawe, J. E. K. Thermochim Acta 2002, 391, 279.
13. Schawe, J. E. K. Thermochim Acta 2002, 388, 299.
14. Cukierman, S.; Halary, J. L.; Monnerie, L. J Non-Cryst Solids 1991, 131, 898.
15. Ellis, B.; Found, M. S.; Bell, J. R. J Appl Polym Sci 1996, 59, 1493.
16. Grillet, A. C.; Galy, J.; Gérard, J. F.; Pascault, J. P. Polymer 1991, 32, 1885.
17. Sauvant, V.; Lauprêtre, F. Polymer 2002, 43, 1259.
18. Mafi, E. R.; Ebrahimi, M. Polym Eng Sci 2008, 48, 1376.
19. Starink, M. J. Thermochim Acta 2003, 404, 163.
20. He, Y. Thermochim Acta 2001, 367, 101.
21. Rosu, D.; Cascaval, C. N.; Mustata, F.; Ciobanu, C. Thermochim Acta 2002, 383, 119.
22. Xu, W.; Bao, S.; Shen, S.; Wang, W.; Hang, G.; He, P. J Polym Sci B Polym Phys 2003, 41, 378.
23. Sbirrazzuoli, N.; Vyazovkin, S.; Mititelu, A.; Sladic, C.; Vincent, L. Macromol Chem Phys 2003, 204, 1815.
24. Vyazovkin, S. Int J Chem Kinet 2002, 34, 418.
25. Popescu, C.; Segal, E. Int J Chem Kinet 1998, 30, 313.
26. Sbirrazzuoli, N. Macromol Chem Phys 2007, 208, 1592.
27. Vyazovkin, S. J Comput Chem 2001, 22, 178.
28. Vyazovkin, S.; Sbirrazzuoli, N. Macromol Rapid Commun 2006, 27, 1515.
29. Maiez-Tribut, S.; Pascault, J. P.; Soule, E. R.; Borrajo, J.; Williams, R. J. J. Macromolecules 2007, 40, 1268.
30. Harrod, J. F. J Polym Sci A Gen Pap 1963, 1, 385.
31. Barral, L.; Cano, J.; López, A. J.; López, J.; Nogueira, P.; Ramírez, C. J Appl Polym Sci 1996, 61, 1553.
32. Boey, F. Y. C.; Qiang, W. J Appl Polym Sci 2000, 78, 511.